ARTICLES

Molecular Mechanism of Anomalous Increase in the Helical Pitch of Cholesteric Liquid Crystals Induced by Achiral Dopants

Masatoshi Kidowaki, Masaya Moriyama, Momoyo Wada, and Nobuyuki Tamaoki*

Molecular Function Group, Institute for Materials & Chemical Process, National Institute of Advanced Industrial Science and Technology (AIST), Tsukuba Central 5, 1-1-1, Higashi, Tsukuba, Ibaraki, 305-8565, Japan

Received: April 8, 2003; In Final Form: September 2, 2003

A dopant-induced anomalous increase in the helical pitch of dicholesteryl 10,12-docosadiynedioate **1** is explained by generation of smectic clusters in the cholesteric phase where the dopants act as promoters of smectic domains. The dopants, having a mesogenic core and the proper length of alkyl chains on both their molecular sides, such as 4,4′-dialkylazobenzenes, 4,4′-dialkylazoxybenzenes and 4,4′-dialkylbiphenyls, considerably increase the pitch. However, dopants having benzene or a binaphthyl structure in the molecular center, an alkyl chain at one side of the molecules and *Z*-isomers of azobenzene and azoxybenzene derivatives, slightly decrease the pitch by acting as impurities that decrease the transition temperature of the host. An X-ray diffraction study of the cholesterics revealed that the pitch increases with an increase in size and amount of the smectic domains induced by the appropriate dopants.

Introduction

Cholesteric liquid crystals (CLCs) have attracted great interest due to their unique macroscopic chirality originating from the helical arrangement of the molecules. The molecular arrangement is spontaneously formed when the mesophasic compounds are intrinsically chiral or are doped with a chiral compound. The helical superstructure of the CLCs is characterized by the helical pitch and handedness. The reflection colors raised by interference of light due to the periodic molecular arrangement are related to the helical pitch through the following equation.

$$\lambda_{max} = pn$$

Here, λ_{max}, p, and n are the wavelength of maximum reflection, the helical pitch length, and the average refractive index, respectively. The helical pitch of the CLC is very sensitive to external stimuli such as temperature, pressure, and electrical and magnetic fields.[1] Due to this nature, the CLC has been intensively studied from both fundamental and application points of view. Such applications include refractive displays,[2] light modulators,[3−5] color recording media,[6,7] and temperature sensors.[8]

In addition to the stimuli mentioned above, a molecule incorporated in the systems as a solute is another important factor contributing to modification of the helical pitch. This effect would be classified roughly into two categories based on the way it affects the helicity of the systems. One is a chirality transfer from a chiral guest to the mesophasic host, as is the typical case with the nematics involving a chiral dopant. Another is an isothermal phase perturbation as typified by depression of the melting point due to impurities. In the former case, although there has been no convincing experimental evidence, the modification of macroscopic chirality would be explained by chiral intermolecular interaction between a chiral solute and its nearest host molecules through modification of both their stackings and conformations.[9−12] When a chiral solute is dissolved in nematics at the limit of a low concentration, the induced helical pitch P is correlated with the concentration C of the solute by the empirical equation.[13,14]

$$P^{-1} = \beta C$$

The proportionality constant β is referred to as the helical twisting power (HTP). In the latter case, an achiral solute in the CLC medium acts as an impurity, resulting in depression of the apparent transition temperature of the systems, leading to isothermal modification of the helical pitch. Therefore, the increase or decrease in the helical pitch depends on the sign of the thermal characteristics (dP/dT) of the host CLCs. The theoretical studies of the thermodynamic properties of nematic systems, which can be applied to cholesterics, have been done by adapting the Flory−Huggins theory with minor modifications.[15−17] The change in the nematic−isotropic phase transition temperature at an infinitely low guest concentration is a function of the heat of transition of the nematic host and the activity coefficient of the dopant in both the nematic and isotropic phases. The strong relevance of thermodynamic properties of the nematics with the size, shape, and chemical nature of the solute molecules has been accounted for in consideration with thermodynamic parameters.[18,19]

Photochemical modification of the macroscopic chirality using photoactive dopants has been extensively investigated,[20] because the systems offer new possibilities in the preparation of optical

* Corresponding author. Tel: +81-29-861-4671. Fax: +81-29-861-4673. E-mail: n.tamaoki@aist.go.jp.

10.1021/jp034916e CCC: $25.00
Published on Web 10/15/2003

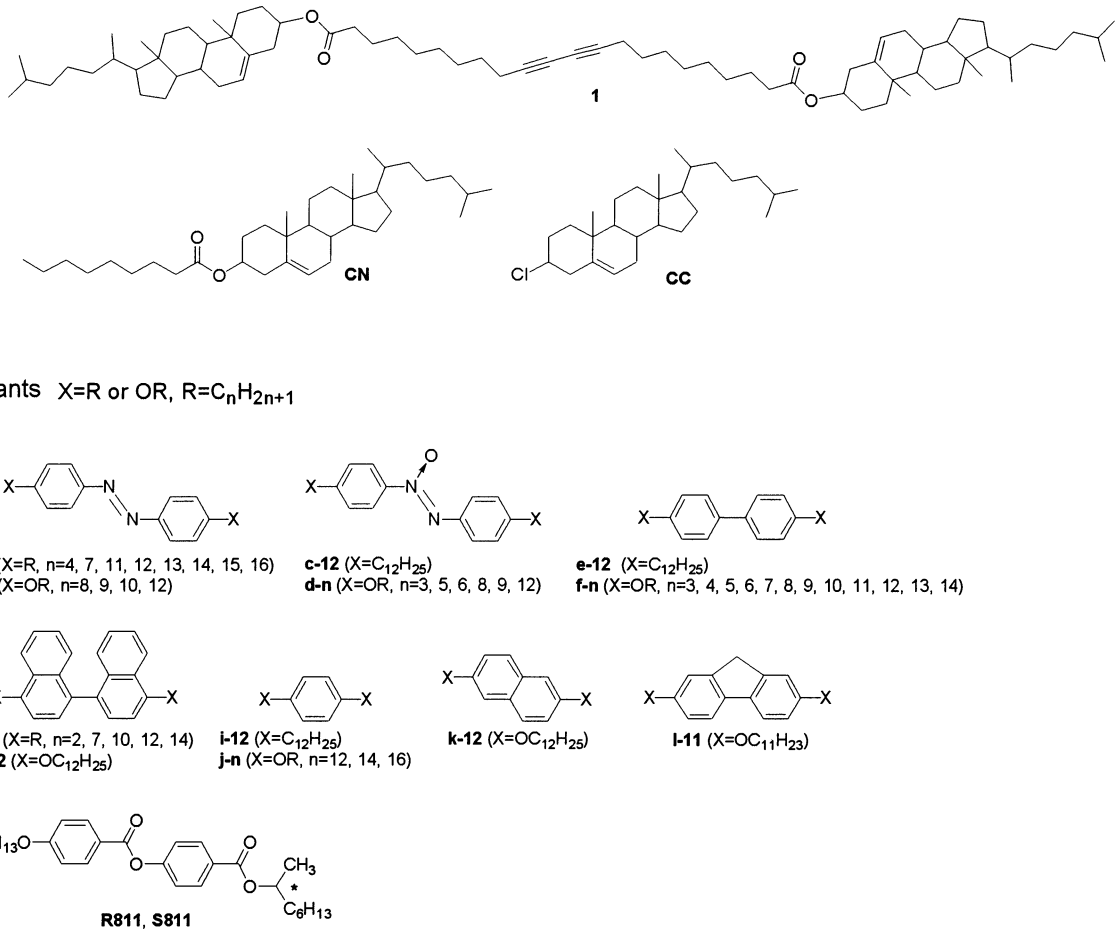

Figure 1. Structures of cholesteric hosts and dopants.

components. In our previous paper,[21−25] we have reported on the specific properties and availability for full color recording devices of glass-forming CLCs. In the course of the study, we have found that addition of a small amount of 4,4′-di-*n*-alkylazobenzene derivatives considerably increases the helical pitch of dicholesteryl docosa-10,12-diyndioate (**1**) and that the variation has a strong correlation with the length of the alkyl chains of azobenzenes and with the ratio of the photoisomers,[24] which is not accounted for by the impurity effect mentioned above.

In this paper, we discuss the mechanism of change in the helical pitch induced by a solute. For this purpose, we employed a variety of dialkyl compounds as solutes including azobenzene, azoxybenzene, biphenyl, binaphthyl, benzene, etc., as shown in Figure 1, and investigated the correlation of the helical pitch with the structure of molecules added to the CLCs. Furthermore, X-ray diffraction studies were conducted to observe the microscopic structure of the CLC systems, and the mechanism of change in the helical pitch induced by the dopants is discussed.

Experimental Methods

General Methods. The NMR spectra were measured by a JEOL GX 270 or LA 600 spectrometer. The transmission spectra were recorded on UV−visible spectrophotometers, Hewlett-Packard 8453. X-ray diffraction patterns were measured using a Rigaku diffractometer (type 4037) with graded d-space elliptical side-by-side multilayer optics, monochromated Cu Kα radiation (40 kV, 30 mA), and an imaging plate (R-Axis IV). The samples were placed in quartz capillary tubes (1.5-mm diameter; 0.01-mm wall thickness) and positioned on a hot stage. The samples were heated to their isotropic phase, subsequently cooled to the mesophase, and then exposed to a radiation beam for 15 s with a 150-mm camera length. A high-pressure mercury lamp (Ushio, 500 W) with appropriate glass filters (for irradiation at 366 nm: Toshiba Glass Co., UV-35 + UVD-36C) was employed as the irradiation source.

Materials. All solvents and reagents were obtained from commercial sources and used without further purification unless otherwise noted.

Cholesteric Liquid Crystals. Preparation of dicholesteryl 10,12-docosadiynedioate **1** was previously reported.[7,24] Cholesteryl chloride (CC) and cholesteryl nonanoate (CN) were purchased and purified through flash column chromatography before using.

Dopants. Azo Derivatives (a−n, b−n, c−n, and d−n). Preparation of 4,4′-dialkylazobenzenes **a**−**n** were previously reported.[7,24] 4,4′-Dialkoxyazoxybenzenes **d**−**n** were obtained commercially. 4,4′-Dialkoxyazobenzenes **b**−**n** were synthesized from 4,4′dihydroxyazobenzene, which was prepared according to the literature.[38]

4-Dodecylazobenzene. To a mixture of 2.5 g (9.6 mmol) of 4-dodecylaniline and 1.2 g (9.8 mmol) of nitrobenzene was added 1.0 g of NaOH over 30 min at 180 °C. After stirring for more 15 min, the mixture was cooled to room temperature and neutralized with dilute hydrochloric acid. The product extracted with ethyl ether was purified through flash chromatography (silica gel, dichloromethane−hexane (1:1)) and recrystallized from ethanol to give 0.92 g (27%) as yellow crystals (mp. 72 °C). ^{1}H NMR($CDCl_3$, 270 MHz) δ 0.68−2.02 (72H, m), 2.21−

2.32 (8H, m), 2.58 (2H, t), 2.69 (2H, t), 4.61(1H, m), 5.37 (1H, m), 7.24 (2H, d), 7.32 (2H, d), 7.84 (2H, d), 7.94 (2H, d). Anal. Calcd. for $C_{24}H_{34}N_2$: C, 82.23; H, 9.78; N, 7.99. Found C, 82.51; H, 9.95; N, 7.77.

4,4′-Dihydroxyazobenzene. This was obtained by recrystallization from ethanol and hexane in 26% yield as reddish brown crystals; mp. 218−219 °C. ^{1}H NMR(DMSO- d_6, 600 MHz) δ 6.90 (4H, d), 7.70 (4H, d), 10.14 (2H, s). Anal. Calcd. for $C_{12}H_{10}N_2O_2 \cdot H_2O$: C, 62.07; H, 5.17; N, 12.07. Found C, 61.89; H, 5.19; N, 11.78.

*4,4′-Di-n-octyloxyazobenzene (**b-8**).* This was prepared from 0.40 g (1.9 mmol) of 4,4′-dihydroxyazobenzene, 0.72 g (3.8 mmol) of 1-*n*-octylbromide, and 0.52 g (3.8 mmol) of K_2CO_3 by means of the Williamson reaction in 8 mL of *N*,*N*-dimethylformamide (DMF) at 75 °C. After stirring for 24 h, the product was extracted with dichloromethane, washed with water, and recrystallized from hexane and ethyl acetate to give 0.39 g (48%) of reddish brown crystals of mp. 99−100 °C. ^{1}H NMR($CDCl_3$, 600 MHz) δ 0.89 (6H, t), 1.25−1.49 (20H, m), 1.78−1.85 (4H, m), 4.03 (4H, t), 6.98 (4H, d), 7.85 (4H, d). Anal. Calcd. for $C_{28}H_{42}N_2O_2$: C, 76.67; H, 9.65; N. 6.39. Found C, 76.56; H, 9.80; N, 6.41.

*4,4′-Di-n-nonyloxyazobenzene (**b-9**).* This was prepared in a way similar to that for **b-8** in 55% yield; mp. 104−105 °C. ^{1}H NMR($CDCl_3$, 600 MHz) δ 0.89 (6H, t), 1.25−1.49 (24H, m), 1.78−1.85 (4H, m), 4.03 (4H, t), 6.98 (4H, d), 7.85 (4H, d). Anal. Calcd. for $C_{30}H_{46}N_2O_2$: C, 77.21; H, 9.93; N. 6.00. Found C, 77.53; H, 10.14; N, 5.99.

*4,4′-Di-n-decyloxyazobenzene (**b-10**).* This was prepared in a way similar to that for **b-8** in 72% yield; mp. 101−102 °C. ^{1}H NMR($CDCl_3$, 600 MHz) δ 0.89 (6H, t), 1.25−1.49 (28H, m), 1.78−1.85 (4H, m), 4.03 (4H, t), 6.98 (4H, d), 7.85 (4H, d). Anal. Calcd. for $C_{32}H_{50}N_2O_2$: C, 77.68; H, 10.19; N, 5.66. Found C, 77.93; H, 10.28; N, 5.60.

*4,4′-Di-n-dodecyloxyazobenzene (**b-12**).* This was prepared in a way similar to that for **b-8** in 81% yield; mp. 107−108 °C. ^{1}H NMR($CDCl_3$, 600 MHz) δ 0.88(6H, t), 1.25−1.49 (36H, m), 1.76−1.87 (4H, m), 4.03 (4H, t), 6.98 (4H, d), 7.85 (4H, d). Anal. Calcd. for $C_{36}H_{58}N_2O_2$: C, 78.49; H, 10.61; N, 5.09. Found C, 78.13; H, 10.46; N, 5.23.

*4,4′-Didodecylazoxybenzene (**c-12**).* The oxidation of **a-12** (0.25 g, 0.48 mmol) with hydrogen peroxide (6.0 mL, 30% aq.) in 4.0 mL of acetic acid and 4.0 mL of chloroform was carried out at 50 °C for 24 h. After the reaction, the product was extracted with chloroform and purified through column chromatography (silica gel, dichloromethane−hexane (1:2)) to give 0.17 g (64%) as a light yellow powder (mp. 122 °C). ^{1}H NMR ($CDCl_3$, 270 MHz) δ 0.82−0.90 (6H, m), 1.20−1.40 (36H, m), 1.58−1.70 (4H, m), 2.60−2.72 (4H, m), 7.24−7.30 (4H, m), 8.12 (2H, d), 8.19 (2H, d). Anal. Calcd. for $C_{36}H_{58}N_2O$: C, 80.84; H, 10.93; N, 5.24. Found C, 81.22; H, 11.06; N, 5.19.

Biphenyl Derivatives (e-12 and f−n). 4,4′-Di-*n*-butyloxybiphenyl **f-4**, 4,4′-di-*n*-heptyloxybiphenyl **f-5** and 4,4′-di-*n*-hexyloxybiphenyl **f-6** were purchased from Tokyo Chemical Industry and used without further purification. The other biphenyl derivatives were synthesized by the coupling reaction between 4,4′-dibromobiphenyl or 4,4′-dihydroxybiphenyl and the corresponding *n*-bromoalkanes.

*4,4′-Di-n-dodecylbiphenyl (**e-12**).* 2.0 g (6.4 mmol) of 4,4′-dibromobiphenyl and a catalytic amount of [1,2-bis(diphenylphosphino)ethane]dichloronickel(II) were suspended in 30 mL of dry ether under a nitrogen atmosphere. To the suspension was added 15 mL of THF solution of dodecylmagnesium bromide, prepared by refluxing 3.2 g (12.8 mmol) of 1-bromododecane and 0.34 g (14.7 mmol) of magnesium in 15 mL of dry ether for 2 h at room temperature. After refluxing for 12 h, the reaction was terminated by the addition of 50 mL of dilute hydrochloric acid, and the product was extracted with 50 mL of ether, washed with a saturated aqueous solution of NaCl and dried over $MgSO_4$. The solvent was removed and the collected solid was recrystallized from acetone to give 1.95 g (62%) of colorless solid of mp. 77−78 °C. ^{1}H NMR ($CDCl_3$, 600 MHz) δ 0.88 (6H, t), 1.25−1.37 (36H, m), 1.61−1.67 (4H, m), 2.63 (4H, t), 7.23 (4H, d), 7.49 (4H, d). Anal. Calcd. for $C_{36}H_{58}$: C, 88.24; H, 11.76. Found C, 88.62; H, 11.73.

*4,4′-Di-n-dodecyloxybiphenyl (**f-12**).* This was prepared from 2.0 g (10.7 mmol) of 4,4′-dihydroxybiphenyl, 5.4 g (21.4 mmol) of 1-dodecylbromide, and 3.0 g (21.4 mmol) of K_2CO_3 by means of the Williamson reaction in 13 mL of DMF at 65 °C. After stirring for 10 h, the product was extracted with dichloromethane, washed with water, and recrystallized from dichloromethane to give 4.9 g (82%) of colorless plate crystals of mp. 114−115 °C. ^{1}H NMR ($CDCl_3$, 600 MHz) δ 0.88 (6H, t), 1.25−1.38 (32H, m), 1.43−1.49 (4H, m), 1.76−1.82 (4H, m), 3.98 (4H, t), 6.93 (4H, d), 7.45 (4H, d). Anal. Calcd. for $C_{36}H_{58}O_2$: C, 88.24; H, 11.76. Found C, 88.62; H, 11.73.

*4,4′-Di-n-heptyloxybiphenyl (**f-7**).* Same procedure as for the synthesis of **f-12**. White plate crystals in 79% yield; mp. 121−122 °C. ^{1}H NMR ($CDCl_3$, 600 MHz) δ 0.90 (6H, t), 1.30−1.38 (12H, m), 1.43−1.49 (4H, m), 1.76−1.82 (4H, m), 3.98 (4H, t), 6.94 (4H, d), 7.46 (4H, d). Anal. Calcd. for $C_{26}H_{38}O_2$: C, 81.62; H, 10.01. Found C, 81.34; H, 9.91.

*4,4′-Di-n-octyloxybiphenyl (**f-8**).* Same procedure as for the synthesis of **f-12**. White plate crystals in 75% yield; mp. 117−118 °C. ^{1}H NMR ($CDCl_3$, 600 MHz) δ 0.89 (6H, t), 1.26−1.38 (20H, m), 1.43−1.49 (4H, m), 1.76−1.82 (4H, m), 3.98 (4H, t), 6.94 (4H, d), 7.46 (4H, d). Anal. Calcd. for $C_{28}H_{42}O_2$: C, 81.90; H, 10.31. Found C, 81.69; H, 10.31.

*4,4′-Di-n-nonyloxybiphenyl (**f-9**).* Same procedure as for the synthesis of **f-12**. White plate crystals in 80% yield; mp. 115−116 °C. ^{1}H NMR ($CDCl_3$, 600 MHz) δ 0.89 (6H, t), 1.26−1.38 (24H, m), 1.43−1.49 (4H, m), 1.76−1.82 (4H, m), 3.98 (4H, t), 6.94 (4H, d), 7.46 (4H, d). Anal. Calcd. for $C_{30}H_{46}O_2$: C, 82.14; H, 10.57. Found C, 81.87; H, 10.48.

*4,4′-Di-n-decyloxybiphenyl (**f-10**).* Same procedure as for the synthesis of **f-12**. White plate crystals in 56% yield; mp. 114−115 °C. ^{1}H NMR ($CDCl_3$, 600 MHz) δ 0.88 (6H, t), 1.26−1.38 (16H, m), 1.43−1.49 (4H, m), 1.76−1.82 (4H, m), 3.98 (4H, t), 6.94 (4H, d), 7.45 (4H, d). Anal. Calcd. for $C_{32}H_{50}O_2$: C, 82.35; H, 10.80. Found C, 82.82; H, 10.81.

*4,4′-Di-n-undecyloxybiphenyl (**f-11**).* Same procedure as for the synthesis of **f-12**. White plate crystals in 18% yield; mp. 115−116 °C. ^{1}H NMR ($CDCl_3$, 600 MHz) δ 0.88 (6H, t), 1.26−1.38 (16H, m), 1.43−1.49 (4H, m), 1.76−1.82 (4H, m), 3.98 (4H, t), 6.94 (4H, d), 7.45 (4H, d). Anal. Calcd. for $C_{34}H_{54}O_2$: C, 82.53; H, 11.00. Found C, 82.75; H, 11.03.

*4,4′-Di-n-tridecyloxybiphenyl (**f-13**).* Same procedure as for the synthesis of **f-12**. White plate crystals in 81% yield; mp. 116−117 °C. ^{1}H NMR ($CDCl_3$, 600 MHz) δ 0.88 (6H, t), 1.25−1.38 (16H, m), 1.43−1.49 (4H, m), 1.76−1.82 (4H, m), 3.98 (4H, t), 6.94 (4H, d), 7.45 (4H, d). Anal. Calcd. for $C_{38}H_{62}O_2$: C, 82.85; H, 11.34. Found C, 83.27; H, 11.37.

*4,4′-Di-n-tetradecyloxybiphenyl (**f-14**).* Same procedure as for the synthesis of **f-12**. White plate crystals in 63% yield; mp. 114−115 °C. ^{1}H NMR ($CDCl_3$, 600 MHz) δ 0.88 (6H, t), 1.25−1.38 (16H, m), 1.43−1.49 (4H, m), 1.76−1.82 (4H, m), 3.98 (4H, t), 6.94 (4H, d), 7.45 (4H, d). Anal. Calcd. for $C_{40}H_{66}O_2$: C, 82.98; H, 11.49. Found C, 83.21; H, 11.45.

Binaphthyl Derivatives (g−n and h-12). The synthesis of 4,4′-diethyl-1,1′-binaphthyl **g-2** was conducted by the catalytic coupling reaction of 1-ethylnaphthalene using $NaNO_2$ with CF_3SO_3H.[39] The synthesis of 4,4′-dialkyl-1,1′-binaphthyls was started from the coupling reaction of 1-bromonaphthalene to afford 1,1′-binaphthyl,[40] and then bromination[41] was conducted with bromine. Alkylation was carried out in the same way as for the dialkylbiphenyls. 4,4′-Didodecyloxy-1,1′-binaphthyl **h-12** was synthesized from 1-dodecyloxynaphthalene with aluminum chloride by means of the Scholl reaction.[42]

*4,4′-Diethyl-1,1′-binaphthyl (**g-2**).* This was obtained in 49% yield as colorless crystals; mp. 106−107 °C. ^{1}H NMR ($CDCl_3$, 600 MHz) δ 1.48 (6H, t), 3.22 (4H, q), 7.26 (2H, dd), 7.40−7.46 (6H, m), 7.49 (2H, dd), 8.15 (2H, d). Anal. Calcd. for $C_{24}H_{22}$: C, 92.86; H, 7.14. Found C, 92.57; H, 7.12.

*4,4′-Diheptyl-1,1′-binaphthyl (**g-7**).* This was obtained in 62% yield as colorless crystals; mp. 106−107 °C. ^{1}H NMR ($CDCl_3$, 600 MHz) δ 0.91 (6H, t), 1.32−1.54 (16H, m), 1.82−1.88 (4H, m), 3.13−318 (4H, m), 7.26−7.28 (2H, m), 7.40−7.51 (8H, m), 8.15 (2H, d). Anal. Calcd. for $C_{34}H_{42}$: C, 90.61; H, 9.39. Found C, 90.45; H, 9.47.

*4,4′-Didecyl-1,1′-binaphthyl (**g-10**).* This was obtained in 16% yield as colorless crystals; mp. 42−43 °C. ^{1}H NMR ($CDCl_3$, 600 MHz) δ 0.89 (6H, t), 1.25−1.54 (28H, m), 1.82−1.88 (4H, m), 3.13−318 (4H, m), 7.26 (2H, dd), 7.39 (2H, d), 7.41−7.43 (4H, m), 7.48 (2H, dd), 8.13 (2H, d). Anal. Calcd. for $C_{40}H_{54}$: C, 89.82; H, 10.18. Found C, 89.58; H, 10.21.

*4,4′-Didodecyl-1,1′-binaphthyl (**g-12**).* This was obtained in 11% yield as colorless crystals; mp. 55−56 °C. ^{1}H NMR ($CDCl_3$, 600 MHz) δ 0.88 (6H, t), 1.25−1.54 (36H, m), 1.82−1.88 (4H, m), 3.13−318 (4H, m), 7.26 (2H, dd), 7.39 (2H, d), 7.41−7.43 (4H, m), 7.48 (2H, dd), 8.13 (2H, d). Anal. Calcd. for $C_{44}H_{62}$: C, 89.43; H, 10.57. Found C, 89.32; H, 10.49.

*4,4′-Ditetradecyl-1,1′-binaphthyl (**g-14**).* This was obtained in 70% yield as colorless crystals; mp. 62−63 °C. ^{1}H NMR ($CDCl_3$, 600 MHz) δ 0.88 (6H, t), 1.25−1.54 (44H, m), 1.82−1.88 (4H, m), 3.13−318 (4H, m), 7.25 (2H, dd), 7.38 (2H, d), 7.41−7.43 (4H, m), 7.48 (2H, dd), 8.13 (2H, d). Anal. Calcd. for $C_{48}H_{70}$: C, 89.10; H, 10.90. Found C, 89.06; H, 10.84.

1-Dodecyloxynaphthalene. Same procedure as for the synthesis of **f-12** under N_2 atmosphere. The product was purified through flash chromatography (silica gel, hexane) to give a colorless liquid in 93% yield. ^{1}H NMR ($CDCl_3$, 600 MHz) δ 0.88 (6H, t), 1.25−1.59 (18H, m), 1.90−1.95 (4H, m), 4.14 (4H, t), 6.80 (1H, d), 7.34−7.49 (4H, m), 7.78 (1H, d), 8.29 (1H, d). Anal. Calcd. for $C_{10}H_{32}O$: C, 84.33; H, 10.32. Found C, 84.33; H, 9.85.

*4,4′-Didodecyloxy-1,1′-binaphthyl (**h-12**).* This was obtained in 18% yield as colorless crystals; mp. 127−128 °C. ^{1}H NMR ($CDCl_3$, 600 MHz) δ 0.89 (6H, t), 1.25−1.47 (36H, m), 1.95−2.00 (4H, m), 4.21 (4H, t), 6.90 (2H, d), 7.28 (2H, dd), 7.34−7.37 (4H, m), 7.44 (2H, dd), 8.38 (2H, d). Anal. Calcd. for $C_{44}H_{62}O_2$: C, 84.83; H, 10.03; O, 5.14. Found C, 84.75; H, 10.05; O, 5.25.

Benzene Derivatives (i-12 and j−n). These compounds were synthesized from 4,4′-dibromobenzene or hydroquinone by methods similar to those for the above-mentioned dialkyl and dialkoxy derivatives.

*4,4′-Di-n-dodecylbenzene (**i-12**).* Colorless solid in 40% yield; mp. 39−41 °C. ^{1}H NMR ($CDCl_3$, 600 MHz) δ 0.89 (6H, t), 1.25−1.33 (36H, m), 1.56−1.60 (4H, m), 2.56 (4H, t), 7.08 (4H, s). Anal. Calcd. for $C_{30}H_{54}$: C, 86.88; H, 13.12, Found C, 87.22; H, 13.70.

*4,4′-Di-n-dodecyloxybenzene (**j-12**).* Colorless solid in 62% yield. mp. 74−75 °C. ^{1}H NMR ($CDCl_3$, 600 MHz) δ 0.88 (6H, t), 1.25−1.46 (36H, m), 1.72−1.76 (4H, m), 3.89 (4H, t), 6.82 (4H, s). Anal. Calcd. for $C_{30}H_{54}O_2$: C, 80.65; H, 12.18; O, 7.16. Found C, 80.45; H, 12.20; O, 7.27.

*4,4′-Di-n-tetradecyloxybenzene (**j-14**).* Colorless solid in 24% yield; mp. 80−81 °C. ^{1}H NMR ($CDCl_3$, 600 MHz) δ 0.88 (6H, t), 1.25−1.46 (44H, m), 1.72−1.76 (4H, m), 3.89 (4H, t), 6.81 (4H, s). Anal. Calcd. for $C_{34}H_{62}O_2$: C, 81.21; H, 12.43. Found C, 81.54; H, 12.60.

*4,4′-Di-n-hexadecyloxybenzene (**j-16**).* Colorless solid in 57% yield; mp. 86−87 °C. ^{1}H NMR ($CDCl_3$, 600 MHz) δ 0.88 (6H, t), 1.25−1.46 (52H, m), 1.72−1.76 (4H, m), 3.89 (4H, t), 6.81 (4H, s). Anal. Calcd. for $C_{38}H_{70}O_2$: C, 81.65; H, 12.62. Found C, 81.498; H, 12.59.

Other Compounds. Chiral agents, **R811** and **S811** (Merck), were used as received. 2,6-Di-*n*-dodecyloxynaphthalene was synthesized by the same procedure as that for the synthesis of **f-12** under N_2 atmosphere. The synthesis of 2,7-di-*n*-undecyloxyfluorene was started from the preparation of 2,7-dihydroxyfluorene and conducted by means of the Williamson reaction.

*2,6-Di-n-dodecyloxynaphthalene (**k-12**).* The product was recrystallized from ethyl acetate to give colorless crystals in 27% yield. mp. 89−90 °C. ^{1}H NMR($CDCl_3$, 600 MHz) δ 0.89-(6H, t), 1.25−1.51(36H, m), 1.80−1.85(4H, m), 4.04(4H, t), 7.08(2H, s), 7.11(2H, d), 7.60(2H, d). Anal. Calcd. for $C_{34}H_{56}O_2$: C, 82.20; H, 11.36. Found C, 82.69; H, 11.36.

2,7-Dihydroxyfluorene. The mixture of 4.8 g (15 mmol) of 2,7-dibromofluorene, 0.25 g (1.7 mmol) of CuBr(I), and 88 mL of NaOH aqueous solution (20%) was sealed into an autoclave and stirred at 230 °C for 6 h. The mixture was allowed to room temperature and filtered. The filtrate was acidified with concentrated H_2SO_4 to afford the precipitate. The collected precipitate was purified through flash chromatography (silica gel, ethyl acetate) to give a light yellow solid in 8.8% yield. ^{1}H NMR (DMSO- d_6, 600 MHz) δ 3.61 (2H, s), 6.71 (2H, d), 6.90 (2H, s), 7.46 (2H, d), 9.25 (2H, s).

*2,7-Di-n-undecyloxyfluorene (**l-11**).* The product was recrystallized from ethyl acetate and hexane to give light yellow crystals in 28% yield; mp. 113−114 °C. ^{1}H NMR ($CDCl_3$, 600 MHz) δ 0.88 (6H, t), 1.25−1.51 (32H, m), 1.77−1.82 (4H, m), 3.81 (2H, s), 3.99 (4H, t), 6.88 (2H, d), 7.05 (2H, s), 7.54 (2H, d). Anal. Calcd. for $C_{35}H_{54}O_2$: C, 82.95; H, 10.74. Found C, 83.32; H, 10.75.

Results and Discussion

General Properties of Cholesteric Films Containing Dopants. Cholesteryl ester **1** containing several wt % of dopants shows a cholesteric phase at 78−116 °C same as pure **1**. At this concentration, the doping hardly affects the transition temperature of **1** at all. The selective reflection color of **1** with or without dopants is easily observed by shear stress inducing the grandjean alignment at their cholesteric temperature. The temperature dependence of the pitch, dP/dT, for all sample films is minus, and the wavelength of the maximum reflection decreases with an increase in temperature, the same as for pure **1**. The films of **1** containing dopants are vitrified by quenching from their cholesteric temperature to 0 °C in ice water. The obtained glassy state of the CLC is sufficiently stable on an experimental time scale at ambient temperature.

Effect of the Center Structure of Dopants on the Pitch. To investigate the effect of the center structure of the dopants on the helical pitch of **1**, we employed compounds substituted with dodecyl groups at either end of the molecules as a dopant.

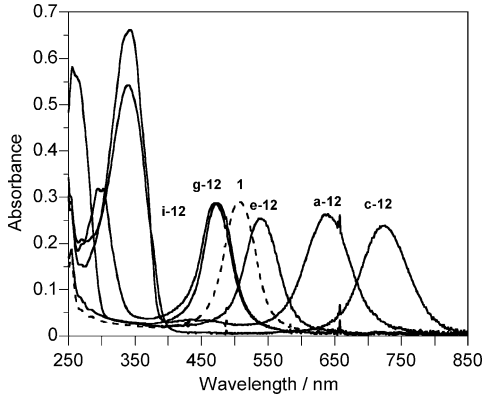

Figure 2. Absorption spectra of the glassy films of pure **1** and **1** containing 2 wt % of **a-12**, **c-12**, **e-12**, **g-12**, and **i-12**, respectively. The films were quenched from 90 °C, and their thickness was controlled by a 5-μm spherical silica spacer.

TABLE 1: Wavelength of UV−Visible Absorption Peaks (λ_{max}) for the Glassy Films[a] (5-μm thickness) of 1 With and Without 2 wt % of a-12, c-12, e-12, g-12, and i-12

	λ_{max}/nm	
dopants	electronic transition	selective reflection
non		507
a-12	343, 442	639
c-12	340	724
e-12	261	540
g-12	295, 302	470
i-12		474

[a] The films were quenched from 90 °C.

Figure 2 shows the UV−visible absorption spectra of the glassy films of **1** with and without 2 wt % of **a-12**, **c-12 e-12**, **g-12**, and **i-12**, respectively. The absorption bands above 400 nm are assigned to the selective reflections due to the helical alignment of the molecules, while those below 400 nm are assigned to the electronic transitions inherent in the dopants. In case of a film containing **a-12**, a weak absorption is observed around 442 nm due to the $n-\pi^*$ forbidden transition, typical for azobenzene derivatives. Their wavelength of absorption maxima, λ_{max}, is summarized in Table 1. λ_{max} due to the selective reflection for the films doped with **a-12**, **c-12**, and **e-12** is observed at 639, 724, and 540 nm, respectively. These values are longer than the 507 nm of pure **1**, indicating that doping of **a-12**, **c-12**, and **e-12** increases the pitch. In the case of **e-12**, although it is difficult to obtain reproducible results because the solubility of **e-12** in the host CLC should be low, the direction of the shift in the reflection band shows the same tendency. On the other hand, doping of **g-12** and **i-12** decreases the pitch; their λ_{max} values are 470 and 474 nm, respectively. The dopants increasing the pitch have a structural resemblance in their rod shape core, whereas those with decreasing pitch have a bulky shape or a small core. In other words, dopants having a mesogenic structure increase the pitch. In the case of **g-12**, we should consider the chiral effect as well as the structural effect due to its axial chirality. However, the chirality effect can be ignored here because **g-12** is a racemic structure. We will discuss the details of this effect later.

The effect is more pronounced when the change in λ_{max} of the reflection bands is expressed as a function of the concentration of the dopants. We extended our survey of dopants to the molecules having alkoxy groups as their side groups and naphthalene (**k-12**) and fluorene (**l-11**) derivatives. The shift in reflection bands is represented by $\Delta\lambda_{max}$ that is obtained by subtracting the λ_{max} of pure **1** from the λ_{max} of **1** with the dopants (Figure 3). The absolute values of $\Delta\lambda_{max}$ increase with an

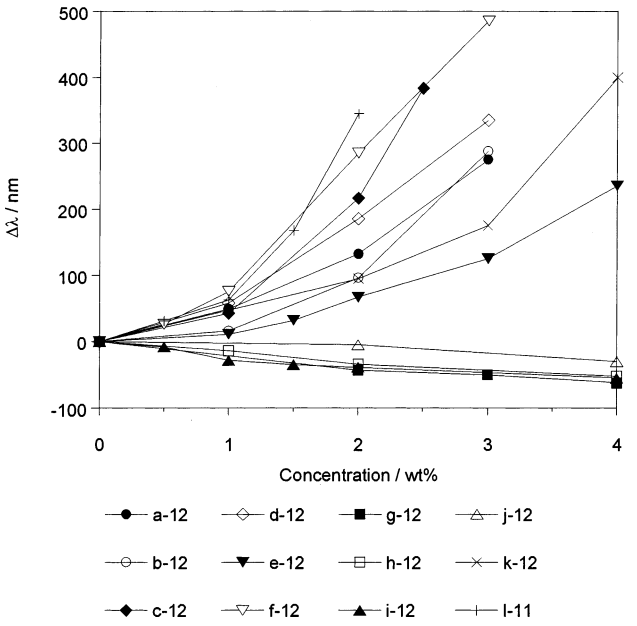

Figure 3. Change in $\Delta\lambda_{max}$ of **1** as a function of the concentration of **a-12**−**l-11**, respectively, at 90 °C.

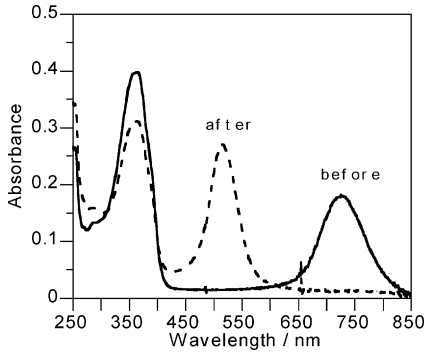

Figure 4. Absorption spectra of a glassy film of **1** containing 2 wt % of **d-12** before and after photoirradiation, respectively. The photoirradiation was performed with a 366-nm light saurce at 90 °C.

increase in the concentration. These dopants are classified into two types, increasing the pitch (**a-12**−**f-12**, **k-12**, and **l-11**) and decreasing it (**g-n**−**j-n**). In the former case, the $\Delta\lambda_{max}$ increases nonlinearly and the difference in $\Delta\lambda_{max}$ among the dopants becomes clear with an increase in the concentration. It should be noted that the shift rises to the near-infrared region at higher concentration and that such large values could not be attained without dopants. In the latter case, the shift in λ_{max} is small compared to the former, even at the higher concentration, and $\Delta\lambda_{max}$ decreases in a monotonic manner. These results indicate that the center structure plays a decisive role in changing the pitch. Corresponding to the structural effect, it may worth pointing out that the photochemical isomerization of the dopants induces a change in the helical pitch as reported for azobenzene derivatives in our previous paper.[24] Exposing a film of **1** including **d-12** to UV-light induces a shift in the reflection band from 725 to 515 nm and a decrease in the electronic transition band (361 nm) of **d-12** (Figure 4). The shorter wavelength shift is induced by the photoisomerization of **d-12** from the *E* to *Z* isomer because the *Z* isomer has a bent core structure.

Effect of Alkyl Chain Length of Dopants on the Pitch. We have investigated the effect of alkyl chain length of the dopants on the pitch of **1**, as shown in Figure 5. Dependence of the chain length is clearly observed for the films of **1** containing **b**−**n**, **d**−**n**, and **f**−**n**, and their plots show maximum

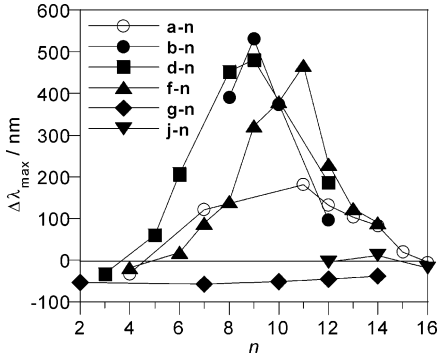

Figure 5. Change in $\Delta\lambda_{max}$ for the films of **1** containing 2 wt % of **a**−**n**,[24] **b**−**n**, **d**−**n**, **f**−**n**, **g**−**n**, and **j**−**n** as a function of the alkyl chain length, *n*, (C_nH_{2n+1}) at 90 °C.

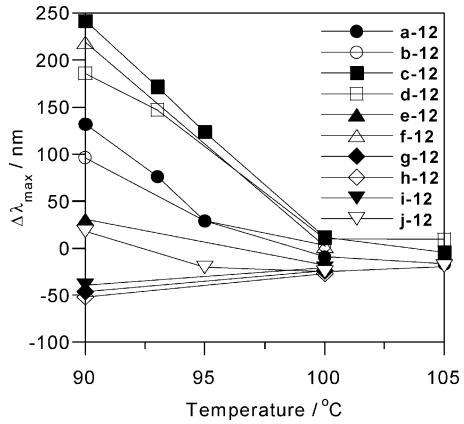

Figure 6. Change in $\Delta\lambda_{max}$ of **1** with 2 wt % of **a-12**−**j-12** as a function of temperature.

values at 9, 9, and 11 of carbon numbers (*n*), respectively. In contrast, the dependence is hardly observed for the films with the dopants (**g**−**n, j**−**n**) which decrease the pitch. The dependence of the pitch on the alkyl chain is not due to the difference in concentration resulting from the difference in their molecular weight. **d-3** and **f-4** decrease in the pitch even though they have mesogenic cores, indicating that the alkyl chain length is an important factor as well as the center structure. It should be mentioned that 4-dodecylazobenzene decreases the pitch, although it has a mesogenic core and a dodecyl group. To increase the pitch, the dopants should have the proper length of alkyl chains at both sides of the molecules.

Effect of Temperature on Doping. The doping-induced variation in λ_{max} at various temperatures is plotted in Figure 6. The absolute values of $\Delta\lambda_{max}$ of all films decrease with an increase in temperature. Above 100 °C, the change in pitch is hardly observed for any cholesteric mixture. The effect of doping on the pitch is apparent below 100 °C. This result shows that the effect of the dopants diminishes with an increase in temperature and has a threshold around 100 °C. Because the threshold temperature is dopant-independent, the temperature depends only on the thermal properties of the host cholesterics.

Effect of Chirality of Dopants. The effect of chiral dopants on the pitch of **1** is shown in Figure 7. **R811** and **S811** are chiral dopants exerting an effect in the opposite direction on the induced cholesteric pitch of nematics, with **R811** having a right-handed and **S811** having a left-handed sense. **R811** increases $\Delta\lambda_{max}$ with an increase in concentration, while **S811** hardly affects the shift in reflection band. The film doped with their racemic mixture shows a small shift to a longer wavelength,

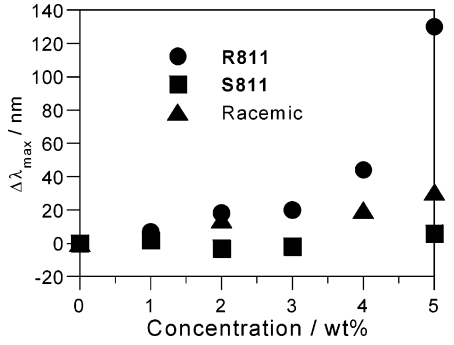

Figure 7. Change in $\Delta\lambda_{max}$ for the films of **1** containing **R811**, **S811**, and their racemic mixture as a function of concentration at 90 °C.

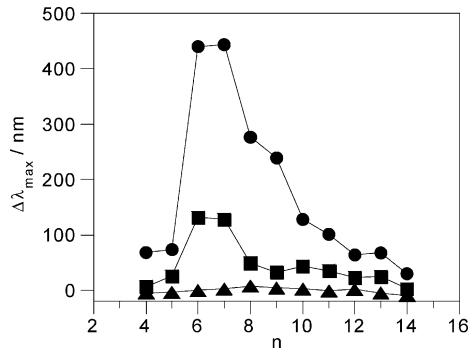

Figure 8. Change in $\Delta\lambda_{max}$ for the cholesteric mixture containing 2 wt % of **f**−**n** as a function of the alkyl chain length at 32 °C (circles), 35 °C (squares), 40 °C (triangles).

the amount of which roughly corresponds to the sum of the shifts due to half portions of each enantiomer. To explain this result, we should consider both chirality and structural effects. These enantiomeric dopants have mesogenic cores and alkyl chains on both sides, which indicates that the dopants increase the pitch of **1** on the basis of the above results from the achiral dopants. In general, to consider the chirality effect, we can adopt the additivity law into the behavior of the pitch. When a chiral dopant induces the same sense as the host cholesterics, their pitch will decrease. Conversely, when the sense is opposite, the pitch will increase. **R811** is a case of the opposite sense, while **S811** is a case of the same sense. **R811** increases the pitch by both structural and chirality effects. However, **S811** hardly affects the pitch due to the opposing effects of the structure and chirality. It is known that when the 3β chain length of the steroid ring system is long enough, the compounds become left-handed cholesterics, such as cholesteryl nonanoate and cholesteryl oleate.[26] The observation of the reflection light with circular polarized plates shows that the samples reflect L-circular polarized light. Circularly polarized light having the same handedness as the cholesterics will be reflected. Therefore, **1** has a left-handed sense, which is consistent with the above explanation of the effect of the chiral dopants.

Doping Effect on Low Molecular Weight Cholesteric Mixture. We conducted a study of dopant-induced change in the pitch with the classical low molecular weight cholesteric mixture of cholesteryl chloride (CC) and cholesteryl nonanoate (CN). We chose the mixing ratio, CC/CN = 18:82 because the mixture shows the reflection bands in the visible region and a negative sign of d*P*/d*T* the same as **1**. The significant dependence of the alkyl chain length of the doped **f**−**n** and temperature on the pitch is observed for the cholesteric mixture (Figure 8) as observed for **1**. The plots at 32 and 35 °C show maximum peaks at carbon number of 7 and 6, respectively. The

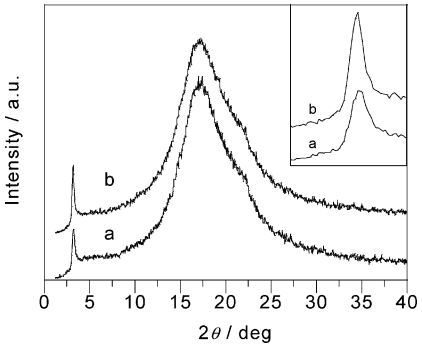

Figure 9. X-ray diffraction patterns for pure **1** (a) and **1** containing 2 wt % of **a-11** (b) at 90 °C. Inset is the magnification of the small angle peaks.

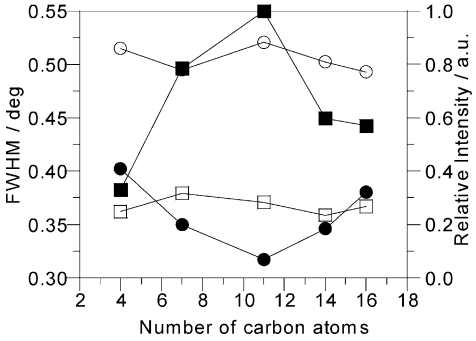

Figure 10. Effect of the alkyl chain length on the half-width (circles) and the relative intensity (squares) of the small-angle X-ray diffraction peaks for **1** containing 2 wt % of **a**−**n** at 90 °C (closed markers) and 110 °C (open markers). The lines are visual guides.

values of $\Delta\lambda_{max}$ decrease with an increase in the temperature. At 40 °C, the dependence of the alkyl chain length is hardly observed. The alkyl chain length of **f**−**n** giving a maximum change in the pitch in the cholesteric mixture CC/CN is shorter than that in **1**.

X-ray Diffraction Study of the Cholesteric Phase. X-ray diffraction patterns of unaligned samples of pure **1** and **1** with 2 wt % of **a-11** are shown in Figure 9. There are major diffraction peaks at two diffraction angles. The broader peaks at 17.1° (d = 5.18 Å) are ascribed to the interaction of neighboring, parallel molecules. The peaks at 3.15° (d = 28.03 Å) would be due to the order parameter fluctuations of the cholesteric regions from and to the smectic-like arrangement, which is termed cybotactic domains.[27−31] The interlayer distances are slightly smaller compared to half of the estimated molecular length of **1** (L = 60.21 Å). The value (d/L = 0.47) suggests that **1** forms an intercalated structure in the transitional smectic clusters.[32,33] The smaller angle peak for **1** containing **a-11** is larger and sharper than that of pure **1**. The sharpness of the peaks can be represented by full widths at half-maximum (fwhm), and the values for pure and doped **1** are 0.414° and 0.325°, respectively. These results indicates that doping of **a-11** promotes the generation of smectic clusters in the cholesterics because the intensity of the peaks depends on the total number of scattering centers in the samples, and the fwhm can be connected with the correlation lengths of the periodic structure by $2/\Delta Q$, where ΔQ is fwhm when the diffraction intensity is plotted as function of the scattering vector Q (= $(4\pi \sin \theta)/\lambda$).[27,30] To obtain further information on the dopant-induced smectic clusters in the cholesterics, X-ray diffraction measurement was performed for **1** containing 2 wt % of azobenzenes, **a**−**n**, at 90 °C and 110 °C. The half width and relative intensity of the smaller angle peaks are plotted as a function of alkyl chain length in Figure 10. A significant dependence of the fwhm and relative intensity on the alkyl chain length is observed for the samples measured at 90 °C, and the values show the minimum and maximum at a carbon number of 11. However, the dependence is not observed for those values measured at 110 °C. These results mean that smectic domains are most pronounced at **a-11** and that the induction of smectic clusters depends on the alkyl chain length of the dopants. This situation (dependence on both temperature and alkyl chain length) is similar to the phenomenon of dopant-induced modification of the helical pitch as mentioned above.

The effect of alkyl chain length of the dopants on both the wavelength of selective reflections and the X-ray peaks of the cholesterics shown in Figures 5 and 10, respectively, offers an explicit relation between the helical pitch and cybotactic clusters. The relation is more clearly shown in Figure 11. The increase

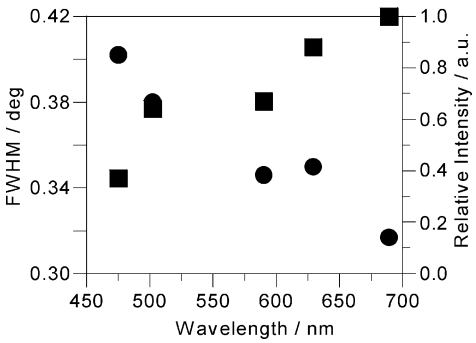

Figure 11. Relation between the wavelength of maximum reflections and the parameters (half-width, circles; and relative intensity, squares) of small-angle X-ray diffraction peaks for **1** containing 2 wt % of **a**−**n** at 90 °C. These data are extracted from the results of Figures 5 and 6.

in λ_{max} brings about an increase in the intensity of the small angle diffraction peaks and a decrease in their half-width. This means that the cholesterics with longer pitch have larger size and a greater number of smectic clusters. In other words, smectic clusters would cause an increase in the helical pitch. There have been some reports mentioning the relationship between the cholesteric pitch and smectic clusters in the cholesterics.[34−37] The anomalous increase in the cholesteric pitch near the cholesteric-smectic transition temperature has been explained by the formation of the smectic clusters. In the present case, the smectic domains are induced by a slight amount of dopants having the proper molecular structure, leading to an anomalous increase in the pitch because the molecules in the smectic clusters align parallel to each other without twisting. It should be stressed that this phenomenon is different from the impurity effect which leads to a change in the phase transition temperature of the host CLCs. The fact that the change in the pitch is very sensitive to alkyl chain length supports this mechanism. The shape and size of the dopants affect their ability to induce smectic clusters because the smectic alignment is a layered structure where the molecules are packed closely and aligned in a parallel manner. In this case, the compatibility of the molecular length between the guest dopants and host cholesterics plays a crucial role. As shown in Figures 5 and 10, **b-9**, **d-9**, and **f-11** have a molecular length causing a strong interaction with **1**, and their estimated molecular lengths show similar values, 32.94, 33.12, and 36.45 Å, respectively. In case of the cholesteric mixture CC/CN, the length of the alkyl chains of **f**−**n** causing a maximum change in the pitch is observed at 6 or 7, and their estimated molecular lengths are 24.25 and 26.52 Å, respectively. It seems that the difference in the molecular length of **f**−**n** giving a maximum change in the pitch between

1 and the cholesteric mixture originates from the difference in their molecular length. The small-angle X-ray diffraction peak due to the smectic-like alignment in the CC/CN mixture is at 3.43° (d = 25.72 Å). This layer distance is slightly shorter than 28.03 Å in **1** and consistent with the molecular length of **f-6** and **f-7**.

Conclusions

These results lead to the conclusion that the dopants with a mesogenic core and the proper length of alkyl chains induce an anomalous increase in the helical pitch of the cholesterics through the induction of smectic clusters. The shift in the reflection band induced by several wt % of dopants reaches the infrared region, which is impossible to obtain for pure host cholesterics. An X-ray diffraction study of the cholesterics elucidated that the doping of appropriate solutes promotes the generation and growth of the domain acting as a smectic core. The increase in both the amount and size of the smectic domains is attributed to the increase in the pitch. The most effective molecular length of the dopants to increase the pitch depends on the host cholesterics, which reflects that the layer structures of the smectic domains mainly consist of host cholesterics.

The information on the mechanism of the dopant-induced change in the cholesteric pitch here is of great importance in molecular modeling to achieve optimum tailored properties of the cholesteric systems.

Acknowledgment. M.K. thanks New Energy and Industrial Technology Development Organization (NEDO) for a fellowship.

References and Notes

(1) Coles, H. In *Handbook of Liquid Crystals*; Demus, D., Goodby, J., Gray, G. W., Spiess, H. W., Vill, V., Eds.; Wiley-VCH: Weinheim, 1998; Vol. 2A, Chapter 4, p 382.
(2) Yang, D. K.; Doane, J. W.; Yaniv, Z.; Glasser, J. *Appl. Phys. Lett.* **1994**, *64*, 1905.
(3) Broer, D. J.; Lub, J.; Mol, G. N. *Nature* **1995**, *378*, 467.
(4) Hikmet, R. A. M.; Kemperman, H. *Nature* **1998**, *392*, 476.
(5) Jacobs, S. D.; Cerqua, K. A.; Marshall, K. L.; Schmid, A.; Guardalben, M. J.; Skerrett, K. J. *J. Opt. Soc. Am. B Opt. Phys.* **1988**, *5*, 1962.
(6) Maxein, G.; Mayer, S.; Zentel, R. *Macromolecules* **1999**, *32*, 5747.
(7) Tamaoki, N.; Parfenov, A. V.; Masaki, A.; Matsuda, H. *Adv. Mater.* **1997**, *9*, 1102.
(8) Gleeson, H. F. In *Handbook of Liquid Crystals*; Demus, D., Goodby, J., Gray, G. W., Spiess, H. W., Vill, V., Eds.; Wiley-VCH: Weinheim, 1998; Vol. 1, Chapter 9, p 823.
(9) Gottarelli, G.; Hibert, M.; Samori, B.; Solladie, G.; Spada, G. P.; Zimmermann, R. *J. Am. Chem. Soc.* **1983**, *105*, 7318.
(10) Gottarelli, G.; Spada, G. P. *Mol. Cryst. Liq. Cryst.* **1985**, *123*, 377.
(11) Gottarelli, G.; Spada, G. P.; Varech, D.; Jacques, J. *Liq. Cryst.* **1986**, *1*, 29.
(12) Gottarelli, G.; Osipov, M. A.; Spada, G. P. *J. Phys. Chem.* **1991**, *95*, 3879.
(13) Baessler, M.; Laronge, T. M.; Labes, M. M. *J. Chem. Phys.* **1969**, *51*, 3213.
(14) Sackmann, E. *J. Am. Chem. Soc.* **1971**, *93*, 7088.
(15) Kronberg, B.; Patterson, D. *J. Chem. Soc., Faraday Trans. 2* **1976**, *72*, 1687.
(16) Kronberg, B.; Glison, D. F. R.; Patterson, D. *J. Chem. Soc., Faraday Trans. 2* **1976**, *72*, 1673.
(17) Luckhurst, G. R.; Gray, G. W. *The Molecular Physics of Liquid Crystals*; Academic Press: London, 1979.
(18) Kronberg, B.; Patterson, D. *J. Chem. Soc., Faraday Trans. 1* **1981**, *77*, 1223.
(19) Croucher, M. D.; Patterson, D. *J. Chem. Soc., Faraday Trans. 1* **1981**, *77*, 1237.
(20) Tamaoki, N. *Adv. Mater.* **2001**, *13*, 1135, and references therein.
(21) Mallia, V. A.; Tamaoki, N. *J. Mater. Chem.* **2003**, *13*, 219.
(22) Tamaoki, N.; Aoki, Y.; Moriyama, M.; Kidowaki, M. *Chem. Mater.* **2003**, *15*, 719.
(23) Moriyama, M.; Tamaoki, N. *Chem. Lett.* **2001**, 1142.
(24) Moriyama, M.; Song, S.; Matsuda, H.; Tamaoki, N. *J. Mater. Chem.* **2001**, *11*, 1003.
(25) Tamaoki, N.; Song, S.; Moriyama, M.; Matsuda, H. *Adv. Mater.* **2000**, *12*, 94.
(26) Kozawaguchi, H.; Wada, M. *Jpn. J. Appl. Phys.* **1975**, *14*, 651.
(27) Albertini, G.; Dubini, B.; Melone, S.; Ponzibossi, M. G. *Mol. Cryst. Liq. Cryst.* **1981**, *70*, 1447.
(28) Bobrovsky, A. Y.; Boiko, N. I.; Shibaev, V. P. *Liq. Cryst.* **2000**, *27*, 57.
(29) De Vries, A. *Mol. Cryst. Liq. Cryst.* **1985**, *131*, 125.
(30) Francescangeli, O.; Laus, M.; Galli, G. *Phys. Rev. E* **1997**, *55*, 481.
(31) McMillan, W. L. *Phys. Rev. A* **1972**, *6*, 936.
(32) Marcelis, A. T. M.; Koudijs, A.; Klop, E. A.; Sudholter, E. J. R. *Liq. Cryst.* **2001**, *28*, 881.
(33) Blatch, A. E.; Fletcher, I. D.; Luckhurst, G. R. *Liq. Cryst.* **1995**, *18*, 801.
(34) Ania, F.; Stegemeyer, H. *Mol. Cryst. Liq. Cryst. Lett.* **1985**, *2*, 67.
(35) Chen, S.; Wu, J. J. *Mol. Cryst. Liq. Cryst.* **1982**, *87*, 197.
(36) Chilaya, G. S.; Lisetski, L. N. *Mol. Cryst. Liq. Cryst.* **1986**, *140*, 243.
(37) Voss, J.; Sackmann, E. *Z. Naturforsch.* **1973**, *28a*, 1496.
(38) Ruslim, C.; Ichimura, K. *J. Mater. Chem.* **1999**, *9*, 673.
(39) Tanaka, M.; Nakashima, H.; Fujiwara, M.; Ando, H.; Souma, Y. *J. Org. Chem.* **1996**, *61*, 788.
(40) Maigrot, N.; Mazaleyrat, J. P. *Synthesis-Stuttgart* **1985**, 317.
(41) Hutchins, L. G.; Pincock, R. E. *J. Org. Chem.* **1980**, *45*, 2414.
(42) Clowes, G. A. *J. Org. Soc. C* **1968**, 2519.